processes

MDPI

Article

Mechanisms of Stress Sensitivity on Artificial Fracture Conductivity in the Flowback Stage of Shale Gas Wells

Xuefeng Yang [1,2], Tianpeng Wu [1,2], Liming Ren [3], Shan Huang [1,2,*], Songxia Wang [1,2], Jiajun Li [1,2], Jiawei Liu [1,2], Jian Zhang [1,2], Feng Chen [3] and Hao Chen [4]

1 Shale Gas Evaluation and Exploitation Key Laboratory of Sichuan Province, Chengdu 610051, China
2 Shale Gas Research Institute, Southwest Oil & Gas Field Company, PetroChina, Chengdu 610051, China
3 Southwest Oil & Gas Field Company, PetroChina, Chengdu 610051, China
4 College of Safety and Ocean Engineering, China University of Petroleum, Beijing 102249, China
* Correspondence: cupbhs@163.com

Abstract: The presence of a reasonable flowback system after fracturing is a necessary condition for the high production of shale gas wells. At present, the optimization of the flowback system lacks a relevant theoretical basis. Due to this lack, this study established a new method for evaluating the conductivity of artificial fractures in shale, which can quantitatively characterize the backflow, embedment, and fragmentation of proppant during the flowback process. Then, the mechanism of the stress sensitivity of artificial fractures on fracture conductivity during the flowback stage of the shale gas well was revealed by performing the artificial fracture conductivity evaluation experiment. The results show that a large amount of proppant migrates, and the fracture conductivity decreases rapidly in the early stage of flowback, and then the decline gradually slows down. When the effective stress is low, the proppant is mainly plastically deformed, and the degree of fragmentation and embedment is low. When the effective stress exceeds 15.0 MPa, the fragmentation and embedment of the proppant will increase, and the fracture conductivity will be greatly reduced. The broken proppant ratio and embedded proppant ratio are the same under the two choke-management strategies. In the mode of increasing choke size step by step, the backflow proppant ratio is lower, and the broken proppant is mainly retained in fractures, so the damage ratio of fracture conductivity is lower. In the mode of decreasing choke size step by step, most of the proppant flows back from fractures, so the damage to fracture conductivity is greater. The research results have important theoretical guiding significance for optimizing the flowback system of shale gas wells.

Keywords: shale gas; flowback system; artificial fracture; stress sensitivity; fracture conductivity

Citation: Yang, X.; Wu, T.; Ren, L.; Huang, S.; Wang, S.; Li, J.; Liu, J.; Zhang, J.; Chen, F.; Chen, H. Mechanisms of Stress Sensitivity on Artificial Fracture Conductivity in the Flowback Stage of Shale Gas Wells. *Processes* **2023**, *11*, 2760. https://doi.org/10.3390/pr11092760

Academic Editors: Zhan Meng, Qingbang Meng and Bin Liang

Received: 29 June 2023
Revised: 28 August 2023
Accepted: 29 August 2023
Published: 15 September 2023

1. Introduction

As a kind of unconventional gas resource, shale gas has been successfully explored and developed, which is an innovation and leap forward in the theory and technology of the global oil and gas industry. The development of shale gas has broken through the understanding of oil and gas geology, expanded the oil and gas development process, guaranteed national energy, and even changed the world oil pattern [1–3]. Shale gas is currently an important support for global natural gas production, but its development faces many more challenges than conventional natural gas. Due to developed micro/nano pores and extremely low permeability, shale reservoirs usually have no natural productivity, so they cannot be developed economically and effectively unless the mode of "horizontal well + volumetric fracturing" is adopted [3]. In the process of shale reservoir fracturing, a large amount of fluid and proppant is injected into the reservoirs, and a complex artificial fracture network is formed to improve the permeability of the shale reservoir [4–7]. Shale gas wells cannot be formally put into production until soaking, flowback, and testing are performed. At the stage of the flowback test, the early productivity of the gas well is

determined by changing the size of the choke. At this stage, the proppant can move in fractures and flow back to the wellbore as fracturing fluid is produced. In this situation, the prop effect weakens, so the fractures close, leading to a reduction in fracture conductivity. In addition, the seepage feature is extremely complex due to the two-phase flow of gas fracturing fluid [8–11]. With the continuous production of fracturing fluid and gas, the pressure in fractures drops gradually, and under the action of overlying pressure, proppant embedment and fragmentation are inevitable. Hence, fracture conductivity decreases greatly and irreversibly, which seriously impacts the estimated ultimate recovery (EUR) of shale gas wells [12,13].

To develop shale gas reservoirs reasonably, it is necessary to determine the stress sensitivity characteristics of artificial fractures and the variation characteristics of fracture conductivity in the stage of the flowback test. Several studies have been conducted on the stress sensitivity characteristics of fractures and the change of fracture conductivity caused by stress sensitivity by means of physical simulation experiments [14–18], numerical simulation [19–22], and theoretical models [23,24]. Zhang [16] used Barnett shale samples to make physical models to study the influence of fracture conductivity under different pressures and proppant concentrations. Computational Fluid Dynamics (CFD) software was used for simulation verification, and the results showed that the conductivity reduction was 45–80%. The fracture property in the study is different from that in the actual reservoir. Tan [17] studied the effect of the layer number and type of proppant on fracture permeability and compressibility, and the backflow of the proppant was not considered. Andrei Osiptsov [20] applied a coupled modeling approach considering fluid displacement in a fracture. The results confirmed that the "smooth" scenario of piece-wise constant choke opening is better because it can maintain fracture conductivity and increase well production. John D. [22] studied the deformation and stability of the proppant in the flowback process by means of the DEM-CFD (Discrete Element Method-Computational Fluid Dynamics) coupling method and the results showed that formation fines and crushed proppant caused permeability damage, reducing the fracture width. Mohammed Kaita [24] developed mathematical models for calculating fracture conductivity, fracture aperture reduction, proppant insertion, and deformation of rod-shaped proppant, and the analysis model can match the embedding and fracture conductivity of rod-shaped proppant under different closing pressures. Seismic methods also have great potential in characterizing fractures and evaluating their conductivity. For instance, Bouchaala used seismic attenuation anisotropy to separate open and closed fractures [25]. Furthermore, Diaz-Acosta combined shear wave splitting and multicomponent velocity analysis to determine fracture orientations in reservoir zones [26]. However, all this research lacked quantitative evaluation on proppant backflow, fragmentation, and embedment. Furthermore, the stress sensitivity characteristics of fractures and the variation characteristics of fracture conductivity under different choke management systems are less researched, so there is no effective guidance for field production.

In this study, a method for evaluating the conductivity of artificial fractures in shale was developed, which can quantitatively evaluate proppant backflow, fragmentation, and embedment. The fracture conductivity evaluation results reveal that the intrinsic conductivity mechanisms vary with the effective stress. The research in this paper provides a theoretical basis for optimizing flowback and production regimes in shale gas wells.

2. Experimental Unit and Method

2.1. Experimental Samples

2.1.1. Core samples

The Wufeng Formation to Long 1_1 Sub-member is currently the major exploration and development formation in the southern Sichuan Basin. The Long1_1 Sub-member is divided into Long $1_1{}^1$, Long $1_1{}^2$, Long $1_1{}^3$, and Long $1_1{}^4$ layers from bottom to top. The Long $1_1{}^1$ to Long $1_1{}^2$ layers have the best production results at present. Therefore, we selected the cores from the Long $1_1{}^1$ to Long $1_1{}^2$ layers as the experimental samples. A core with a diameter

of 2.5 mm was drilled along the bedding direction. Then, the Brazilian splitting method was used to create a fracture in the core. Subsequently, the cores were laid flat after the fractures were filled with proppant quantitatively. Finally, the cores were covered with thermal shrinkable film, and fractures and proppant were fixed. In this experiment, the proppant concentration was 2.0 kg/m^3, and the fracture width after proppant placement was 2.0 mm. The concentration error of proppant placement is less than 0.5%.

2.1.2. Experimental Fluid

The slickwater provided by the oil company was used as the experimental fluid in this study.

2.2. Experimental Unit and Process

Previously, we established an experimental method to test the stress sensitivity of artificial fractures in shale [18]. To further study the mechanisms of stress sensitivity on artificial fracture conductivity in the flowback stage, we have upgraded the experimental unit and methods. The new experimental unit mainly includes the physical modeling system of core holding and proppant backflow, ISCO pump, intermediate container, pressure acquisition system, flow rate acquisition system, and back pressure control system (Figure 1).

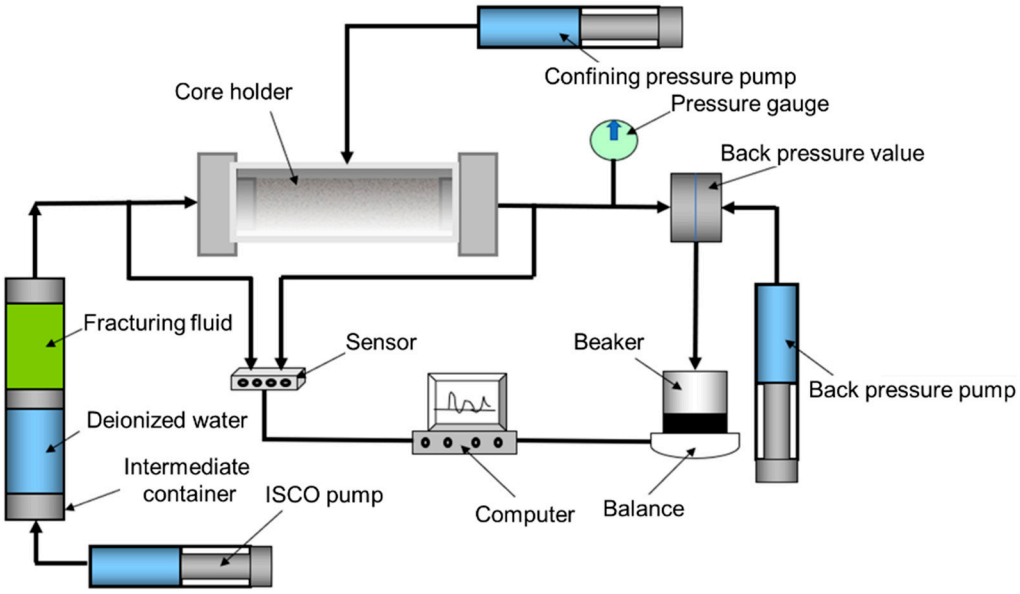

Figure 1. Experimental unit for long-term fracture conductivity.

Figure 2 shows the independently developed physical modeling system of core holding and proppant backflow, which can simulate the long-term conductivity of artificial fractures in shale while collecting the backflow proppant, so as to calculate the backflow proppant ratio. There is a cavity at the exit of the traditional core holding system. This cavity is divided into three structures. The structure I is funnel-shaped, which collects the backflow proppant in the process of fracturing fluid flowback. Structure II is used as a flow channel. Structure III is an enlarged cavity, which traps the backflow proppant to ensure that the position of the proppant will not change greatly with the flow of fracturing fluid after it flows back and facilitates its collection and measurement after the experiment. The maximum pressure of the system is 70 MPa. The flow rate accuracy and the pressure accuracy are 0.5% FS.

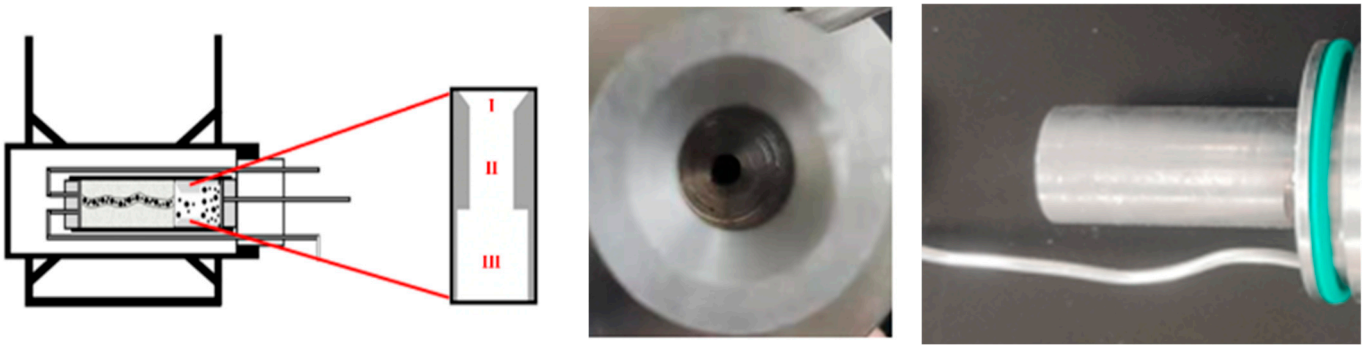

(**a**) (**b**) (**c**)

Figure 2. The physical modeling system of core holding and proppant backflow and its photo. (**a**) Core holder; (**b**) top view of the proppant collection device; (**c**) side view.

It can be known from the field process parameters that the variable flow pressure test method can reflect the actual production process more accurately when the proppant concentration is higher than 1 kg/m^3 [16]. Therefore, in this paper, the variable flow pressure method was adopted, and the confining pressure was used to simulate the overlying pressure, which was kept constant during the experiment. Back pressure was set at the exit of the core, and it was changed to realize the change of the effective stress on cores and simulate the change of different flow pressures in the production process.

2.3. Experimental Data Processing

2.3.1. Calculation of Fracture Conductivity

The internal structure of an artificial fracture can be regarded as a porous medium composed of proppant. The fracture conductivity can be calculated based on the upstream and downstream displacement pressure of the core sample, the flow rate of fluid through the core sample, fluid viscosity, core length, and core diameter. The calculation formula is:

$$\eta = k{\cdot}d_f = \frac{10Q\mu L}{d\Delta P} \quad (1)$$

where $\eta = k{\cdot}d_f$ is fracture conductivity, D·cm; Q is the flow rate of fluid through the core, cm^3/s; μ is fluid viscosity under the test conditions, mPa·s; L is core length, cm; d is core diameter, cm; ΔP is difference between upstream and downstream pressure of the core, MPa.

2.3.2. Calculation of Backflow Proppant, Embedded Proppant, and Broken Proppant Ratios

After the experiment was completed, the core was taken out, and the collection part of the physical modeling system of proppant flowback was removed. After that, the cavity was flushed, and the backflow proppant was collected. The backflow proppant was put into the thermostat oven for drying and then weighed, and the backflow proppant ratio was calculated. Then, the core sample was cut slowly and put into the thermostat oven for drying. The proppant was brushed gently. After the unembedded proppant was collected, the embedded proppant was brushed down and weighed, and the embedded proppant ratio was calculated. Finally, after all the proppant was put on the screen of 120 mesh and shaken for 5 min, the broken proppant was collected and weighed, and the broken proppant ratio was calculated (Table 1).

Table 1. Calculation method of backflow proppant ratio, embedded proppant ratio, and broken proppant ratio.

Parameter	Definition	Formula
Backflow proppant ratio	Percentage of backflow proppant	$\alpha = \frac{m_2}{m_1}$
Broken proppant ratio	Percentage of broken proppant	$\beta = \frac{m_3}{m_1}$
Embedded proppant ratio	Percentage of embedded proppant	$\gamma = \frac{m_4}{m_1}$

Note: α is the backflow proppant ratio, %; β is the broken proppant ratio, %; γ is the embedded proppant ratio, %; m_1 is the mass of proppant in fractures, g; m_2 is the mass of backflow proppant, g; m_3 is the mass of broken proppant, g; m_4 is the mass of embedded proppant, g.

3. Results and Discussion

3.1. Effect of Effective Stresses

Based on the new evaluation method, we studied the variation characteristics of long-term fracture conductivity under different effective stresses and quantitatively evaluated the backflow proppant ratio, broken proppant ratio, and embedded proppant ratio under different stress conditions. To research the variation characteristics of fracture conductivity at different effective stresses, five groups of long-term fracture conductivity experiments were carried out by setting the confining pressure at 30.0 MPa to simulate the overlying pressure and the flow pressure at 0, 5.0, 10.0, 15.0, and 20.0 MPa, corresponding to effective stress of 30.0, 25.0, 20.0, 15.0, and 10.0 MPa, respectively. Figure 3 shows the change in the flow conductivity of artificial fractures in shale over time at different effective stresses. The long-term fracture conductivity drops quickly in the early stage and then slowly, for a large amount of proppant migrates in the early stage. The cores before and after the experiment at the effective stress of 10.0 MPa were CT scanned (see Figure 4). It was found that proppant was obviously absent at the edge of the core after the experiment, indicating that proppant flows back with the flow of fracturing fluid. The proppant at the edge of the core sample flows back to the backflow cavity of the device under the action of lateral drag force (see Figure 5). The same phenomenon was also observed in the stress sensitivity experiments in the previous research conducted by Chen [18].

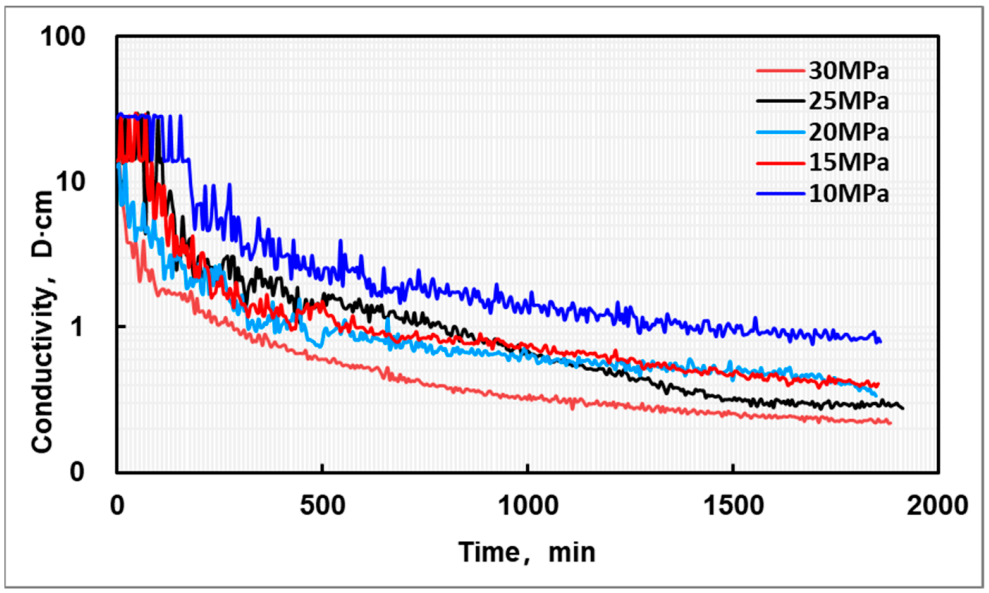

Figure 3. Long-term conductivity of artificial fracture at different effective stresses.

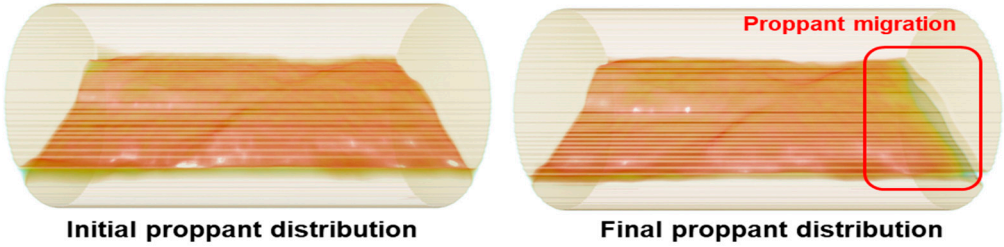

Figure 4. Proppant migration monitored by CT scanning (confining pressure 30 MPa; flow pressure 20 Mpa; flow direction from left to right; there is much less proppant at the exit after the experiment). (**a**) Before the experiment. (**b**) After the experiment.

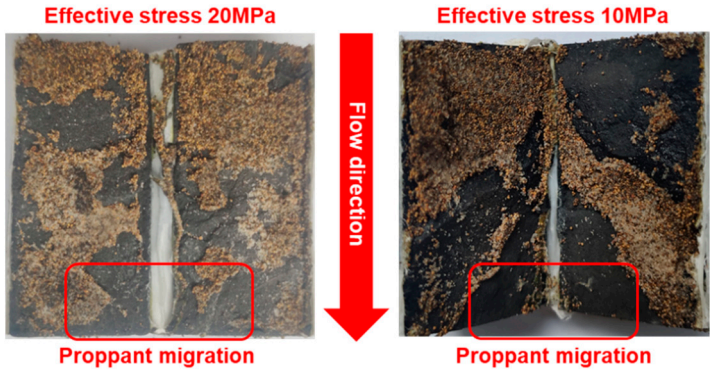

Figure 5. Distribution of proppant on fracture surface under different effective stress (The confining pressure is 30 MPa, and the flow pressures in the left and right figures are 20 MPa and 10 MPa, respectively).

The calculation formula of the conductivity damage ratio is:

$$\varepsilon = \frac{\eta_0 - \eta_i}{\eta_0} \tag{2}$$

where ε is the damage ratio, dimensionless; η_0 is the initial conductivity, D·cm; η_i is the conductivity under different effective stress, D·cm.

Figure 6 shows the damage ratio of the flow conductivity of the artificial fracture in shale at different effective stresses. When the effective stress is 10.0 MPa, the damage ratio of fracture conductivity is only 87.92%. After the effective stress exceeds 15.0 MPa, the damage ratio rises sharply. As the effective stress rises to 25.0 MPa, the damage ratio rises to 93.45%. With the further increase in the effective stress, the damage ratio is unchanged.

To further discuss the influence of proppant migration, fragmentation, and embedment on fracture conductivity, the backflow, embedded, and broken proppant were collected and screened after the experiment, and the broken proppant ratio, embedded proppant ratio and backflow proppant ratio at different effective stresses were calculated, seeing Figure 7. With the increase in the effective stress, the amount of backflow proppant decreases, while the fragmentation and embedment degrees increase greatly. When the effective stress is 10.0 MPa, the proppant mainly suffers plastic deformation, and the fragmentation degree and the embedment degree are lower (embedded proppant ratio 8.43% and broken proppant ratio 3.95%). However, it still can act as a better support. The backflow proppant ratio is higher (20.79%), but the fracture compaction degree is lower, so the fracture conductivity remains higher (0.79 D·cm). After the effective stress reaches or exceeds the critical proppant breaking pressure, a large amount of proppant begins to break and the broken proppant ratio rises quickly. When the effective stress reaches 30.0 MPa, the embedded proppant ratio is 22.79%, the broken proppant ratio is 14.54%, and the support effect of the proppant weakens significantly. The backflow proppant ratio decreases greatly (5.14%), but fracture compaction is obvious due to high effective stress, so the decreasing

amplitude of the fracture conductivity is larger. Eventually, the fracture conductivity is only 0.29 D·cm.

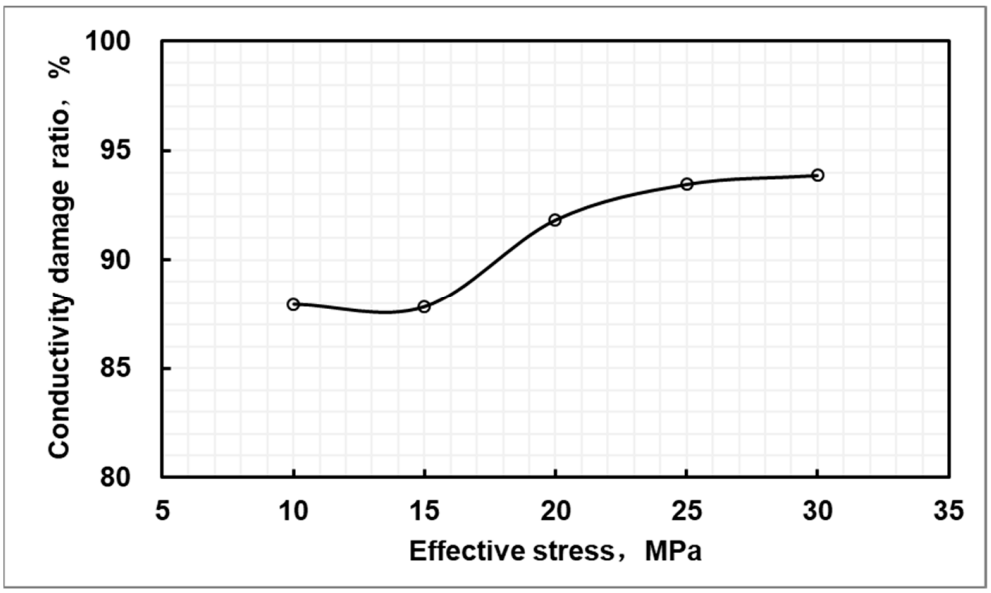

Figure 6. Damage ratio of fracture conductivity at different effective stresses.

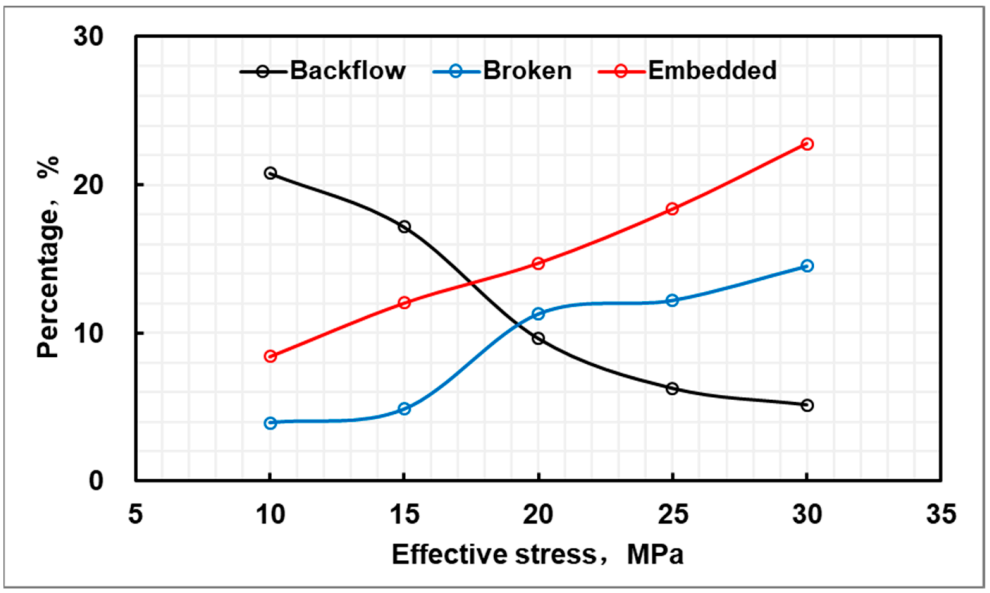

Figure 7. Broken proppant ratio, embedded proppant ratio, and backflow proppant ratio under different confining pressure conditions.

3.2. Effect of the Choke Management System

When different chokes are adopted, the effective stress on fractures is different. The smaller the choke size, the higher the bottom hole flow pressure, and the lower the effective stress on fractures. With the increase in the choke size, the bottom hole flow pressure decreases gradually, and the effective stress on fractures increases gradually. The process of gradually increasing and decreasing the choke size is simulated by gradually increasing and decreasing the effective stress.

3.2.1. Step-by-Step Enlargement of the Choke Size

The confining pressure was fixed at 30.0 MPa, and the flow pressure was gradually decreased from 20.0 MPa to 0 MPa with an interval of 5.0 MPa, whose corresponding effective stress was 10.0, 15.0, 20.0, 25.0, and 30.0 MPa. The displacement at each pressure point lasted for about 720 min.

Figure 8 shows the variation characteristics of fracture conductivity and effective fracture width with the increase in the choke size. In the initial stage, the effective stress on fractures is lower and the immobilization of the proppant to fracture plane is weaker, so the proppant is carried out of fractures by fracturing fluid. Under the action of effective stress, the fractures close and the effective fracture width decreases, leading to a quick decrease in the fracture conductivity. When the effective stress rises to 15.0 MPa, the effective fracture width decreases from 2.0 mm to 0.65 mm, and the fracture conductivity decreases from 1.93 D·cm to 0.24 D·cm. With the increase in the effective stress, the immobilization of the proppant to fracture plane becomes stronger gradually, so little proppant can flow back, and thus fragmentation and embedment increase. As a result, the decreasing amplitudes of effective fracture width and fracture conductivity decrease gradually. When the effective stress rises to 25.0 MPa, the effective fracture width is 0.41 mm and the fracture conductivity is only 0.11 D·cm.

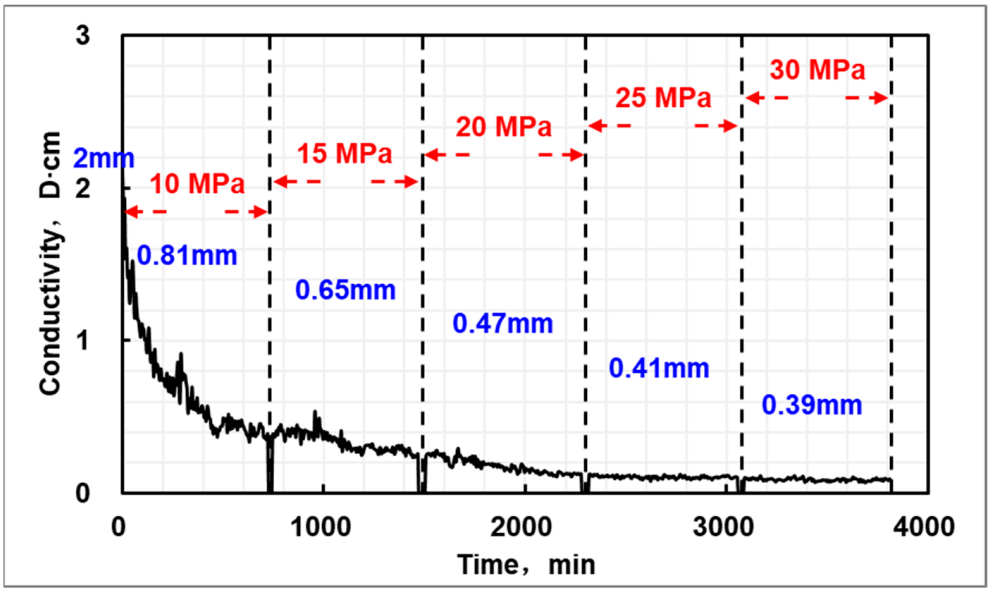

Figure 8. Fracture conductivity vs. time in the process of choke size increasing step by step.

It should be noted that only one core was adopted for simulation in the experiment of increasing choke size step by step. The displacement pressure difference in the experiment rose quickly from 0.71 MPa to 3.28 MPa with the increase in the effective stress. However, in the fracture conductivity experiment of multiple cores at different effective stresses (Section 2.1), the displacement pressure difference rose slowly from 0.23 MPa to 1.23 MPa (see Figure 9). In two experiments, the displacement pressure difference increases. When the effective stress is low, the displacement pressure difference in the experiment of increasing choke size step by step is close to the value in the experiment with different effective stresses. With the increase in the effective stress, the displacement pressure difference in both experiments increases, but the increasing amplitude in the experiment of increasing choke size step by step is larger, so at high effective stress, the displacement pressure difference in the two experiments is obviously different. The main reason is that, when only one core is adopted in the experiment, the damage to the core is accumulated, which means the damage to the core in the stage of low effective stress is accumulated to the damage at high effective stress. Furthermore, the displacement time is longer, and the amount of

displacement fluid is greater. As a result, the fracture surface and proppant are immersed more, and the core is damaged more seriously. In the fracture conductivity experiment of multiple cores at different effective stresses, each core feeds back only the damage under one certain pressure condition.

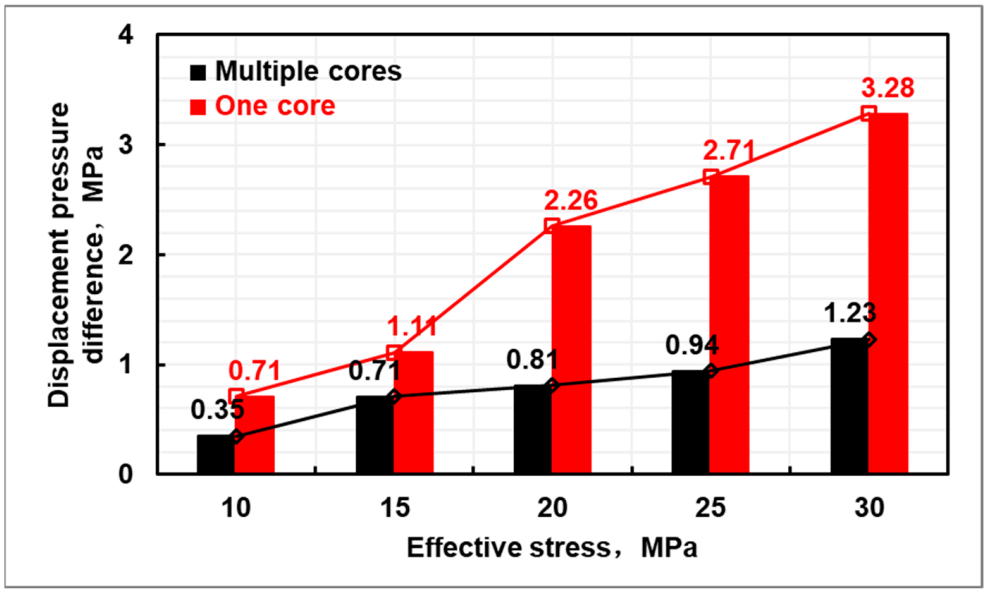

Figure 9. Comparison of the displacement pressure difference between the experiment of choke size increasing step by step and the experiment at different effective stresses.

3.2.2. Step-by-Step Reduction in the Choke Size

The confining pressure was fixed at 30.0 MPa, and the flow pressure was increased from 0 MPa to 30.0 MPa step by step with an interval of 5.0 MPa, whose corresponding effective stress was 30.0, 25.0, 20.0, 15.0, and 10.0 MPa. The displacement at each pressure point lasted for about 720 min.

Figure 10 shows the variation characteristics of fracture conductivity in the process of decreasing choke size step by step. In the initial stage, the effective stress is 30 MPa, the backflow degree of the proppant is weaker, the fragmentation degree and the embedment degree are higher, and most fractures are closed, so the fracture conductivity decreases quickly from 9.46 D·cm to 0.46 D·cm. After 755 min, the effective stress is decreased to 20 MPa by regulating the flow pressure, and the fracture conductivity is recovered to 1.09 D·cm. Afterwards, the fracture conductivity decreases slowly to 0.28 D·cm in the displacement process. Later, the effective stress is decreased to 20, 15, and 10 MPa at the moment of 1570, 2290, and 3055 min, respectively, and the fracture conductivity increases to 1.28, 1.40, and 1.30 D·cm, correspondingly. As the displacement continues, the fracture conductivity decreases slowly to about 0.50 D·cm. The reason for this phenomenon is that, with the decrease the effective stress, fractures are opened again, and thus the fracture conductivity increases. And then, as proppant is carried out of fractures, the support effect becomes weak, so the fractures close again and the fracture conductivity decreases again. It is indicated that, in the process of decreasing choke size step by step, fractures receive more damage of stress sensitivity in the early stage, and later when the effective stress is decreased, the fracture conductivity recovers gradually but the recovery capacity is extremely limited.

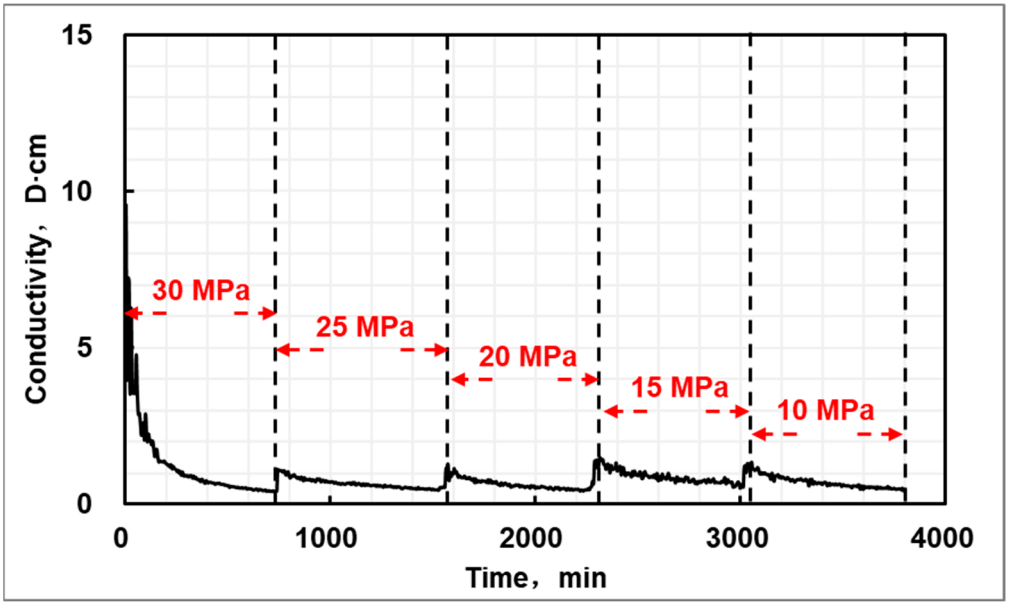

Figure 10. Fracture conductivity vs. time in the process of decreasing choke size step by step.

3.2.3. Comparison of Different Choke Management Systems

The results of two groups of fracture conductivity experiments are normalized to further compare the change characteristics of long-term conductivity under different choke management systems (see Figure 11). The calculation formula of the normalized conductivity is:

$$\overline{\eta}_i = \frac{\eta_i}{\eta_{max}} \tag{3}$$

where $\overline{\eta}_i$ is the normalized conductivity, dimensionless; η_i is the fracture conductivity at different times, D·cm; η_{max} is the maximum fracture conductivity, D·cm.

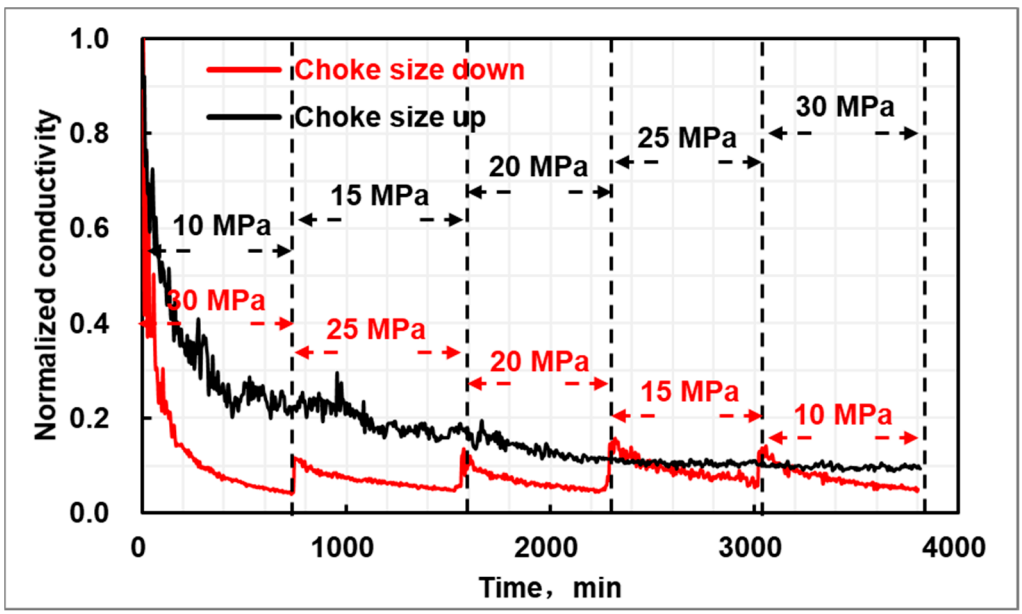

Figure 11. Conductivity vs. time under different choke management systems.

The damage to fractures accumulates and increases gradually as the choke size (the effective stress) increases. When the effective stress is increased to 30.0 MPa, the normalized conductivity is only 0.10. When the choke size is decreased step by step, the normalized

fracture conductivity decreases quickly to 0.04 at the effective stress of 30.0 MPa. With the decrease in the effective stress, the normalized conductivity increases quickly and then decreases slowly. When the effective stress is 10.0 MPa, the normalized conductivity is only 0.05, which is much lower than the value in the mode of increasing choke size step by step. To sum up, if the objective external conditions are not taken into consideration, as for the same reservoir, the reservoir damage is increased gradually in the flowback test mode of increasing choke size step by step, but the fracture conductivity is always higher than the value in the mode of decreasing choke size. In the mode of decreasing choke step by step, the initial reservoir damage is stronger, and later with the decrease in the effective stress, the fracture conductivity can be recovered in a way, but the recovery capacity is limited. As the production goes on, the fracture conductivity will continue to decrease.

Two choke size adjustment modes are obviously different in the changing trend of the conductivity damage ratio caused by fracture stress sensitivity. Figure 12 shows that, in the flowback test mode of increasing choke size step by step, the damage ratio of fracture conductivity is 78% when the initial effective stress is 10.0 MPa. As the effective stress rises to 20.0–25.0 MPa, the damage ratio increases to about 90%. With the further increase in the effective stress, the damage ratio of fracture conductivity is basically unchanged. The process of increasing choke size step by step is the increasing process of effective stress, and its damage to fractures is accumulated and increased gradually. In the early stage, the effective stress is low, so the backflow of proppant leads to a quick increase in damage ratio. In the late stage, the effective stress is high and proppant fragmentation and embedment are dominant, so the increasing amplitude of the damage ratio is not large. In the mode of decreasing choke size step by step, the damage ratio of fracture conductivity is as high as 96% when the initial effective stress is 30 MPa. As the effective stress is decreased to 20 MPa, the damage ratio decreases to about 94%. With the further decrease in the effective stress, the damage ratio is basically maintained at 94% and can be hardly recovered. In the early stage, the effective stress is high enough to bring unrecoverable damage to reservoirs. With the decrease in the effective stress in the late stage, the fracture conductivity recovers slightly in a short period, but it will decrease quickly.

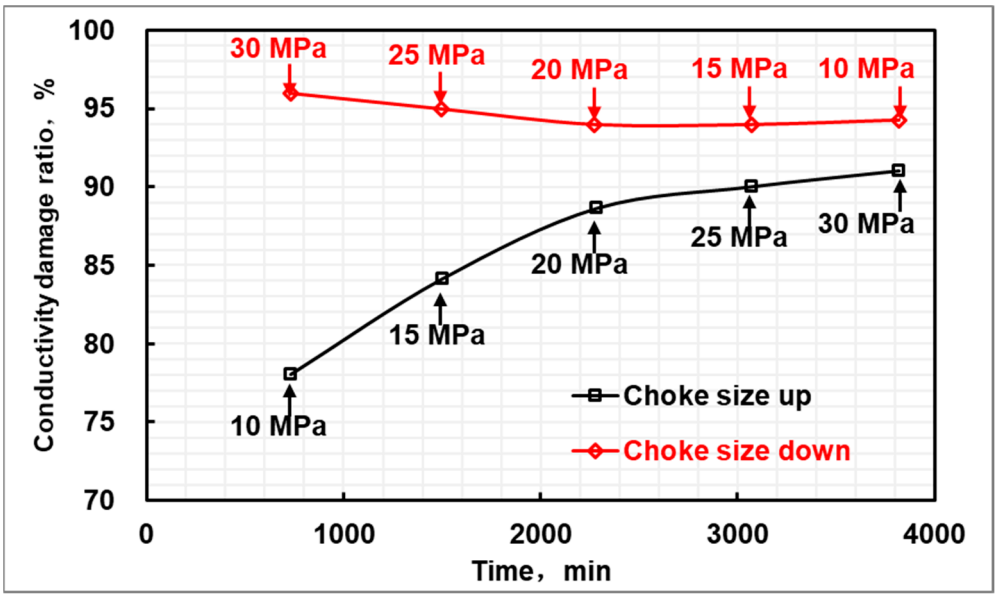

Figure 12. Conductivity damage ratio under different choke management systems.

To compare the characteristics of proppant backflow, embedment, and fragmentation under different choke management systems, the backflow proppant ratio, broken proppant ratio, and embedded proppant ratio were statistically calculated and analyzed after each group of experiments (see Figure 13). In the process of increasing choke size, the effective stress on fractures is lower in the initial stage, the proppant fragmentation and embedment

are weaker, and the immobilization of proppant is also weaker, so proppant tends to flow back. The backflow proppant is mainly unbroken, and the backflow proppant ratio is 7.90%. In the process of decreasing choke size step by step, the effective stress on fractures is higher in the initial stage, so the proppant can hardly flow and fragmentation and embedment are dominant. Subsequently, as the effective stress decreases, the fracture opens, and the proppant begins to migrate. The migration degree is high, up to 12.17%, because the proppant has been broken. The displacement time is long, and the amount of displacement fluid and the effective stress are basically similar. Hence, the broken proppant ratio and embedded proppant ratio in the two choke adjustment modes are relatively close. It should be noted that in the experiment of increasing choke size step by step, the broken proppant is mainly retained in fractures. In the experiment of decreasing choke size step by step, the broken proppant is mainly in the "cavity" of the holder, which means it flows back from fractures.

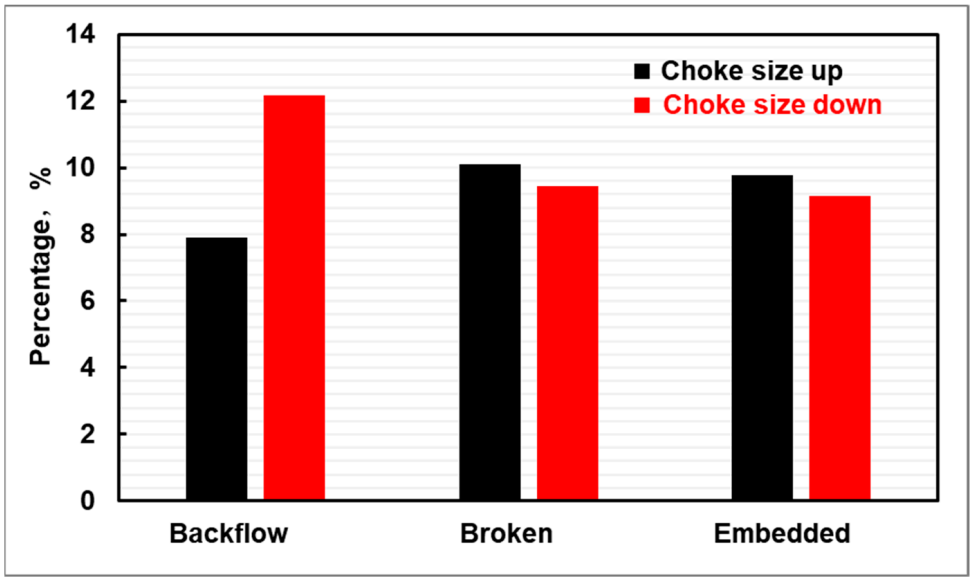

Figure 13. Influence of different choke management systems on support effect of proppant.

4. Conclusions

In this paper, we proposed a new method for evaluating the flow conductivity of artificial fractures in shale and developed a new type of core holder which can quantitatively evaluate the amount of proppant backflow, embedment, and fragmentation. In addition, the mechanisms of stress sensitivity on fracture conductivity under different choke adjustment modes were revealed. The main conclusions are as follows.

(1) The proppant backflow is dominant and proppant fragmentation and embedment degrees are low when the effective stress is lower. After the effective stress exceeds 15.0 MPa, proppant backflow reduces, and fragmentation and embedment degrees increase.

(2) In the mode of increasing choke size step by step, with the increase in the effective stress, the damage to fracture conductivity increases gradually. In the mode of decreasing choke size step by step, the effective stress is the largest and the damage ratio of fracture conductivity is the highest at the initial moment. With the gradual decrease in the effective stress, fracture conductivity is recovered in a way, but the recovery capacity is limited. And as production goes on, fracture conductivity will continue to decrease.

(3) The broken proppant ratio and embedded proppant ratio are basically the same in both modes. In the mode of increasing choke size step by step, the backflow proppant ratio is lower, the broken proppant is mainly retained in fractures and the damage ratio of fracture conductivity is lower. In the mode of decreasing choke size step by step, most of the broken proppant flows back from fractures and the damage to fracture conductivity is greater.

(4) The influence of stress sensitivity on the production of shale gas wells can be minimized by adopting the mode of increasing choke size step by step in the stage of the flowback test.

Author Contributions: Conceptualization, X.Y.; Methodology, T.W. and S.W.; Investigation, L.R. and J.Z.; Data curation, J.L. (Jiawei Liu); Writing—original draft, S.H., J.L. (Jiajun Li), F.C. and H.C. All authors have read and agreed to the published version of the manuscript.

Funding: This research was funded by the Science and Technology Project of CNPC (2023ZZ21).

Data Availability Statement: The data presented in this study are available on request from the corresponding author.

Conflicts of Interest: The authors declare no conflict of interest.

References

1. Ma, X.; Xie, J. The Progress and Prospects of Shale Gas Exploration and Development in Southern Sichuan Basin, SW China. *Pet. Explor. Dev.* **2018**, *45*, 172–182. [CrossRef]
2. Ma, X.; Li, X.; Wan, Y.; Shi, Q.; Wang, Y.; Zhang, X.; Che, M.; Guo, W.; Guo, W. Dominating Factors on Well Productivity and Development Strategies Optimization in Weiyuan Shale Gas Play, Sichuan Basin, SW China. *Pet. Explor. Dev.* **2020**, *47*, 594–602. [CrossRef]
3. Ma, X. Enrichment Laws and Scale Effective Development of Shale Gas in the Southern Sichuan Basin. *Nat. Gas Ind. B* **2019**, *6*, 240–249. [CrossRef]
4. He, X.; Li, W.; Dang, L.; Huang, S.; Wang, X.; Zhang, C.; Qiao, Z.; Chen, Y. Key Technological Challenges and Research Directions of Deep Shale Gas Development. *Nat. Gas Ind.* **2021**, *41*, 118–124.
5. Huang, S.; Li, W.; Wu, J.; Zhang, H.; Luo, Y. A Study of the Mechanism of Nonuniform Production Rate in Shale Gas Based on Nonradioactive Gas Tracer Technology. *Energy Sci. Eng.* **2020**, *8*, 2648–2658. [CrossRef]
6. Huang, S.; Ma, X.; Yang, H.; Wu, J.; Zhang, J.; Zhao, S.; Zhang, D.; Ren, C.; Huang, L. Experimental Characterization and Molecular Modeling of Kerogen in Silurian Deep Gas Shale from Southern Sichuan Basin, China. *Energy Rep.* **2022**, *8*, 1497–1507. [CrossRef]
7. Huang, S.; Ma, X.; Yong, R.; Wu, J.; Zhang, J.; Wu, T. Transient Interporosity Flow in Shale/Tight Oil Reservoirs: Model and Application. *ACS Omega* **2022**, *7*, 14746–14755. [CrossRef]
8. Li, Y.; Luo, H.; Li, H.; Liu, X.; Tan, Y.; Chen, S.; Cai, J. A Brief Review of Dynamic Capillarity Effect and Its Characteristics in Low Permeability and Tight Reservoirs. *J. Pet. Sci. Eng.* **2020**, *189*, 106959. [CrossRef]
9. Li, Y.; Luo, H.; Li, H.; Chen, S.; Jiang, X.; Li, J. Dynamic Capillarity during Displacement Process in Fractured Tight Reservoirs with Multiple Fluid Viscosities. *Energy Sci. Eng.* **2020**, *8*, 300–311. [CrossRef]
10. Yan, G.; Li, Z.; Galindo Torres, S.A.; Scheuermann, A.; Li, L. Transient Two-Phase Flow in Porous Media: A Literature Review and Engineering Application in Geotechnics. *Geotechnics* **2022**, *2*, 32–90. [CrossRef]
11. Yan, G.; Li, Z.; Bore, T.; Torres, S.A.G.; Scheuermann, A.; Li, L. A Lattice Boltzmann Exploration of Two-Phase Displacement in 2D Porous Media under Various Pressure Boundary Conditions. *J. Rock Mech. Geotech. Eng.* **2022**, *14*, 1782–1798. [CrossRef]
12. Karantinos, E.; Sharma, M.M.; Ayoub, J.A.; Parlar, M.; Chanpura, R.A. Choke-Management Strategies for Hydraulically Fractured Wells and Frac-Pack Completions in Vertical Wells. *SPE Prod. Oper.* **2018**, *33*, 623–636. [CrossRef]
13. Bagci, S.; Stolyarov, S. Flowback Production Optimization for Choke Size Management Strategies in Unconventional Wells. In Proceedings of the SPE Annual Technical Conference and Exhibition, OnePetro, Calgary, AB, Canada, 30 September–2 October 2019.
14. Qingzhi, W. Influence of Proppant Embedment on Fracture Long-Term Flow Conductivity. *Nat. Gas Ind.* **2005**, *25*, 65.
15. Lei, W. Experimental Research on Long-Term Conductivity of the Proppant Combination with Different Grain Sizes in Complex Fracturing. *Nat. Gas Ind.* **2005**, *25*, 64.
16. Zhang, J.; Ouyang, L.; Hill, A.D.; Zhu, D. Experimental and Numerical Studies of Reduced Fracture Conductivity Due to Proppant Embedment in Shale Reservoirs. In Proceedings of the SPE Annual Technical Conference and Exhibition, SPE, Amsterdam, The Netherlands, 27–29 October 2014; p. SPE-170775.
17. Tan, Y.; Pan, Z.; Liu, J.; Feng, X.-T.; Connell, L.D. Laboratory Study of Proppant on Shale Fracture Permeability and Compressibility. *Fuel* **2018**, *222*, 83–97. [CrossRef]
18. Chen, H.; Zhou, T.; Fan, H.; Zhang, J.; Yang, S. Preparation method and stress sensitivity of shale reservoir rock sample with artificial fractures. *Acta Pet. Sin.* **2020**, *41*, 1117–1126.
19. Guotao, W.; Yun, X.; Zhenzhou, Y.; Lifeng, Y.; Jing, Z. Numerical Simulation Considering the Impact of Proppant and Its Embedment Degree on Fracture Flow Conductivity. *Nat. Gas Ind.* **2013**, *33*, 65–68.
20. Osiptsov, A.; Garagash, I.; Boronin, S.; Tolmacheva, K.; Lezhnev, K.; Paderin, G. Impact of Flowback Dynamics on Fracture Conductivity. *J. Pet. Sci. Eng.* **2020**, *188*, 106822. [CrossRef]

21. Deng, S.; Li, H.; Ma, G.; Huang, H.; Li, X. Simulation of Shale–Proppant Interaction in Hydraulic Fracturing by the Discrete Element Method. *Int. J. Rock Mech. Min. Sci.* **2014**, *70*, 219–228. [CrossRef]
22. Zhu, H.; Shen, J.; Zhang, F.; Huang, B.; Zhang, L.; Huang, W.; McLennan, J.D. DEM-CFD Modeling of Proppant Pillar Deformation and Stability during the Fracturing Fluid Flowback. *Geofluids* **2018**, *2018*, 3535817. [CrossRef]
23. Chen, D.; Ye, Z.; Pan, Z.; Zhou, Y.; Zhang, J. A Permeability Model for the Hydraulic Fracture Filled with Proppant Packs under Combined Effect of Compaction and Embedment. *J. Pet. Sci. Eng.* **2017**, *149*, 428–435. [CrossRef]
24. Jia, L.; Li, K.; Zhou, J.; Yan, Z.; Wan, F.; Kaita, M. A Mathematical Model for Calculating Rod-Shaped Proppant Conductivity under the Combined Effect of Compaction and Embedment. *J. Pet. Sci. Eng.* **2019**, *180*, 11–21. [CrossRef]
25. Bouchaala, F.; Ali, M.Y.; Matsushima, J.; Bouzidi, Y.; Takougang, E.M.T.; Mohamed, A.A.; Sultan, A. Azimuthal investigation of compressional seismic-wave attenuation in a fractured reservoir. *Geophysics* **2019**, *84*, 437–446. [CrossRef]
26. Diaz-Acosta, A.; Bouchaala, F.; Kishida, T.; Jouini, M.S.; Ali, M.Y. Investigation of fractured carbonate reservoirs by applying shear-wave splitting concept. *Adv. Geo-Energy Res.* **2023**, *7*, 99–110. [CrossRef]